Acta Pharmacologica Sinica

www.nature.com/aps

ARTICLE

Small molecule IVQ, as a prodrug of gluconeogenesis inhibitor QVO, efficiently ameliorates glucose homeostasis in type 2 diabetic mice

Ting-ting Zhou[1], Tong Zhao[2], Fei Ma[3], Yi-nan Zhang[2], Jing Jiang[2], Yuan Ruan[2], Qiu-ying Yan[2], Gai-hong Wang[3], Jin Ren[3], Xiao-wei Guan[2], Jun Guo[2], Yong-hua Zhao[4], Ji-ming Ye[5], Li-hong Hu[2], Jing Chen[3] and Xu Shen[2]

Gluconeogenesis is a major source of hyperglycemia in patients with type 2 diabetes mellitus (T2DM), thus targeting gluconeogenesis to suppress glucose production is a promising strategy for anti-T2DM drug discovery. In our preliminary in vitro studies, we found that a small-molecule (E)-3-(2-(quinoline-4-yl)vinyl)-1H-indol-6-ol (QVO) inhibited the hepatic glucose production (HGP) in primary hepatocytes. We further revealed that QVO suppressed hepatic gluconeogenesis involving calmodulin-dependent protein kinase kinase β- and liver kinase B1-adenosine monophosphate-activated protein kinase (AMPK) pathways as well as AMPK-independent mitochondrial function-related signaling pathway. To evaluate QVO's anti-T2DM activity in vivo, which was impeded by the complicated synthesis route of QVO with a low yield, we designed and synthesized 4-[2-(1H-indol-3-yl)vinyl]quinoline (IVQ) as a prodrug with easier synthesis route and higher yield. IVQ did not inhibit the HGP in primary hepatocytes in vitro. Pharmacokinetic studies demonstrated that IVQ was quickly converted to QVO in mice and rats following administration. In both *db/db* and *ob/ob* mice, oral administration of IVQ hydrochloride (IVQ-HCl) (23 and 46 mg/kg every day, for 5 weeks) ameliorated hyperglycemia, and suppressed hepatic gluconeogenesis and activated AMPK signaling pathway in the liver tissues. Furthermore, IVQ caused neither cardiovascular system dysfunction nor genotoxicity. The good druggability of IVQ has highlighted its potential in the treatment of T2DM and the prodrug design for anti-T2DM drug development.

Keywords: type 2 diabetes mellitus; hepatic gluconeogenesis; AMPK signaling pathway; (E)-3-(2-(quinoline-4-yl)vinyl)-1H-indol-6-ol (QVO); 4-[2-(1H-indol-3-yl)vinyl]quinoline (IVQ); prodrug

Acta Pharmacologica Sinica (2019) 40:1193–1204; https://doi.org/10.1038/s41401-018-0208-2

INTRODUCTION

Diabetes mellitus (DM) is a chronic disease with high morbidity and mortality [1]. Type 2 diabetes mellitus (T2DM), accounting for over 90% of DM cases, is a chronic metabolic disease with a complex pathogenesis that is characterized by insulin resistance, pancreatic β-cell dysfunction, and elevated glucose production [2]. Physiologically, the liver has a pivotal role in maintaining glucose homeostasis, and hepatic gluconeogenesis is stimulated to maintain the blood glucose level in the normal range during prolonged starvation [3], while uncontrolled regulation of gluconeogenesis is believed to be one of the major factors leading to metabolic disorders [2]. Accumulated evidence has demonstrated that gluconeogenesis is a main source of continuous hepatic glucose production (HGP) in the diabetic condition, contributing to 50%–60% of the elevated glucose level in T2DM patients [1]. Therefore, targeting gluconeogenesis inhibition is a promising strategy for anti-diabetic drug discovery.

Adenosine monophosphate-activated protein kinase (AMPK), as a major energy sensor, functions potently in maintaining glucose homeostasis of the whole body, including skeletal muscles, adipose tissues, pancreatic islets, and the liver [4, 5]. Structurally, AMPK is a heterotrimeric complex with one catalytic α subunit and two regulatory units β and γ, containing two isoforms of α (α1 and α2) and β (β1 and β2), and three isoforms of γ subunits (γ1, γ2, and γ3) [6, 7]. It is activated by elevated AMP upon energy shortage, causing inhibition of the ATP-consuming anabolic process and stimulation of the ATP-producing process [4]. AMPK activity can be directly regulated by AMP binding to the regulatory γ subunit or indirectly by phosphorylating the catalytic α subunit on Thr172 through other kinases, including calmodulin-dependent protein kinase kinase β (CaMKKβ) and liver kinase B1 (LKB1) [5]. AMPK inactivation is associated with several metabolic disorders, including T2DM, obesity and insulin resistance [5]. Because of its crucial role in maintaining energy homeostasis, AMPK is always accepted as a potent target for drug development against metabolic disease [7].

In the current study, we found that the small-molecule (E)-3-(2-(quinoline-4-yl)vinyl)-1H-indol-6-ol (QVO; Fig. 1a) inhibited

[1]Wuxi School of Medicine, Jiangnan University, Wuxi 214122, China; [2]State Key Laboratory Cultivation Base for TCM Quality and Efficacy, School of Medicine and Life Sciences, Nanjing University of Chinese Medicine, Nanjing 210023, China; [3]Shanghai Institute of Materia Medica, Chinese Academy of Sciences, Shanghai 201203, China; [4]Institute of Chinese Medical Sciences, University of Macau, Macau, China and [5]School of Health and Biomedical Sciences, RMIT University, PO Box 71, Melbourne, VIC 3083, Australia
Correspondence: Li-hong Hu (lhhu@njucm.edu.cn) or Jing Chen (jingchen@simm.ac.cn) or Xu Shen (xshen@njucm.edu.cn)
These authors contributed equally: Ting-ting Zhou and Tong Zhao

Received: 23 May 2018 Accepted: 23 December 2018
Published online: 4 March 2019

hepatic gluconeogenesis in primary hepatocytes according to the screening platform against the laboratory in-house compound library. In addition, we identified that 4-[2-(1H-indol-3-yl) vinyl]quinoline (IVQ), as a prodrug of QVO, could be converted to QVO in vivo, and IVQ hydrochloride (IVQ-HCl) effectively suppressed hepatic gluconeogenesis and ameliorated glucose homeostasis in T2DM model mice. IVQ-HCl decreased fasting blood glucose and glycated hemoglobin (HbA1c) levels and improved glucose and pyruvate tolerance in both *db/db* and *ob/ob* mice. Moreover, IVQ exerted no obvious cardiovascular system dysfunction or apparent genotoxicity, suggesting the potential druggability of IVQ. Mechanistic studies have demonstrated that QVO probably suppressed gluconeogenesis involving the CaMKKβ- and LKB1-AMPK pathways and AMPK-independent mitochondrial function-related signaling pathway. Our current work has highlighted the promising strategy of targeting gluconeogenesis inhibition and the potential of IVQ in the treatment of T2DM.

MATERIALS AND METHODS

Materials and reagents

Glucagon, STO609, and 3-(4,5-dimethyl-2-thiazolyl)-2,5-diphenyl-2-H-tetrazolium bromide (MTT) were purchased from Sigma-Aldrich (Shanghai, China). QVO was obtained from a commercial compound library (SPECS, Zoetermeer, Netherlands). IVQ-HCl was prepared as indicated in the Supplementary Materials section. Antibodies against phospho-AMPK (Thr172), AMPK and LKB1 were from Cell Signaling Technology (MA, USA), and glyceraldehyde-3-phosphate dehydrogenase (GAPDH) was from Kangcheng Biotech (Shanghai, China). The antibody against phospho-TORC2 (Ser171) was obtained from Bioss Antibodies, Inc. (MA, USA). LKB1-siRNA and AMPK-siRNA were purchased from Thermo Scientific (MA, USA). Lipofectamine RNAiMAX and all media for cell culture, fetal bovine serum and antibiotic supplements were from Invitrogen (CA, USA).

Cell culture

Primary hepatocytes were isolated from nine-week-old male C57BL/6 mice using a two-step collagenase perfusion method as previously described [8]. Freshly isolated mouse hepatocytes were cultured in Williams' E medium supplemented with 10% FBS, 100 U/mL of penicillin, and 100 mg/mL of streptomycin.

HGP and q-PCR assays

HGP and q-PCR assays were conducted as described previously [8]. For the HGP assay, hepatocytes were treated with serum-free MEM containing the corresponding compounds and glucagon (10 nM) for 16 h. The cells were then incubated with compounds and glucagon (10 nM) in glucose production detection buffer (glucose-free DMEM without phenol red supplemented with sodium lactate (20 mM) and sodium pyruvate (2 mM)) for 6 h. Detection buffer was collected to detect the glucose level using a colorimetric glucose assay kit (Nanjing Jiancheng, Nanjing, China). The primers for q-PCR were obtained from Sangon Biotech (Shanghai, China) and were as follows:

G6Pase (+): 5'-TAATTGGCTCTGCCAATGGCGATC-3';
G6Pase (−): 5'-ATCAGTCTGTGCCTTGCCCCTGT-3';
PEPCK (+): 5'-CTGCATAACGGTCTGGACTTC-3';
PEPCK (−): 5'-CAGCAACTGCCCGTACTCC-3';
GAPDH (+): 5'-ACAGCAACAGGGTGGTGGAC-3';
GAPDH (−): 5'-TTTGAGGGTGCAGCGAACTT-3'.

AMPK enzymatic activity assay

Recombinant AMPK activity was assessed using a modified non-radioactive approach as published previously [9]. Briefly, recombinant-AMPK α2β1γ1 (400 ng/mL, Invitrogen) was pre-incubated with QVO (20 μM) or A-769662 (1 μM) for 30 min on ice. The kinase reaction was initiated upon adding ATP (50 μM) and substrate SAMS (100 μM; Sangong, Shanghai, China) at room temperature for 30 min, avoiding light. The generation of ADP reflected AMPK enzyme activity, and ADP was detected by the ADP Hunter Plus assay kit (Discover X, CA, USA). The fluorescent signal was detected using an M5 multi-detection reader (Molecular Devices, CA, USA) at an excitation wavelength of 530 nm and an emission wavelength of 590 nm.

Western blot assay

Western blot assays were performed as previously described [10]. Briefly, cell lysates were separated by SDS-PAGE and were transferred to nitrocellulose membranes (GE Health, CHI, USA). The membranes were incubated with the corresponding primary antibodies at 4 °C overnight and were subsequently incubated with secondary antibodies for 2 h at room temperature. Visualization of the signals on the membranes was obtained using the ImageQuant LAS 4000 mini system (GE Health) and West-Dura detection system (Thermo Scientific).

ATP and MMP assays

ATP and MMP assays were performed as previously described [11]. For the ATP assay, hepatocytes were incubated with QVO (1, 10, 20 μM) for 4 h. The concentration of ATP was detected using the ATP assay kit (Beyotime Company, S0027, Shanghai, China) according to the manufacturer's protocol.

The mitochondrial membrane potential (MMP) level was detected using the MMP assay kit with JC-1 (Beyotime Company, C2006) according to the manufacturer's instructions. The hepatocytes were incubated with the corresponding compounds for 4 h and then were incubated with JC-1 (10 μg/mL) for 20 min at 37 °C. After washing twice with JC-1 buffer, the fluorescent signal was detected using an M5 multi-detection reader at 490/530 (ex/em) and 525/590 (ex/em). The data were shown as the relative ratio between the red fluorescent signal and green fluorescent signal.

MTT assay

The cells were incubated with different concentrations of QVO (1, 10, 20 μM) for 24 h, followed by the addition of 200 μL of DMSO to dissolve the formazan crystals after incubation with MTT (0.5 mg/mL) at 37 °C for 4 h. The absorbance at 490 or 570 nm was measured using an M5 spectrophotometer (Molecular Devices).

Seahorse assay

Hepatocytes were seeded at 5000 cells/well in MEM with 10% FBS and 1% penicillin-streptomycin in XF96 cell culture microplates (Seahorse Biosciences, CA, USA) overnight. The cells were starved for 4 h with MEM containing QVO (1, 10, 20 μM) or metformin (2 mM, as a positive control). Next, the cells were cultured in 175 μL of XF assay base medium (HCO_3^- free-modified DMEM (Seahorse Bioscience) supplemented with 1 mM *L*-glutamine and 1 mM pyruvate) at 37 °C with no CO_2 supplementation for 1 h to allow temperature and pH equilibration, followed by measurement of the baseline cellular respiration using the Seahorse XF96 instrument (Seahorse Bioscience). This device detected the oxygen consumption rate (OCR) in 96-well plates after sequentially adding to each well 25 μL of the corresponding compounds, an ATP coupler (oligomycin, 1 μM), an uncoupling agent [carbonyl cyanide 4-(trifluoromethoxy) phenylhydrazone (FCCP), 0.5 μM], and a mixture of antimycin A (1 μM) and rotenone (1 μM) according to the instructions of the Seahorse XF Cell Mito Stress kit (Seahorse Biosciences).

Mitochondrial respiratory complex activity assay

Mitochondria were obtained as described previously [12]. Briefly, hepatocytes were harvested, and cell pellets were homogenized in buffer A (83 mM sucrose, 10 mM Mops, pH = 7.2). The same volume

of buffer B (250 mM sucrose, 30 mM Mops) was added to the sample, and the homogenate was centrifuged at 1000 × *g*/min for 5 min. The supernatant was then re-centrifuged at 12 000 × *g*/min for 2 min to obtain the mitochondrial fraction. The mitochondria were suspended in buffer D (1 M 6-aminohexanoic acid, 50 mM Bis-Tris·HCl, pH = 7.0) after washing in buffer C (320 mM sucrose, 1 mM EDTA, 10 mM Tris·HCl, pH = 7.4). The highly enriched mitochondrial fractions were used to detect the activity of mitochondrial respiratory complexes using the mitochondrial respiratory chain complex I (NADH dehydrogenase), complex II (succinate dehydrogenase), complex III (cytochrome *c* reductase), complex IV (cytochrome *c* oxidase), and complex V (mitochondrial F0F1-ATP synthase) activity assay kits (GENMED, Shanghai, China) with the M5 spectrophotometer. Complex I was measured as rotenone-sensitive NADH-CoQ reductase by monitoring the oxidation of NADH at 340 nm in the presence of coenzyme Q. Complex II was measured at 600 nm by succinate-mediated phenazine methosulfate reduction of dichloroindophenol by succinate dehydrogenase. Complex III was measured at 550 nm by succinate-mediated cytochrome *c* reduction. Complex IV was measured by the oxidation of reduced cytochrome *c* at 550 nm. Complex V was measured as oligomycin-sensitive ATP synthase by monitoring the oxidation of NADH at 340 nm in the presence of pyruvate.

Animal experiments

All animals received humane care, and all animal-related protocols were approved by the Institutional Animal Care and Use Committees at Shanghai Institute of Materia Medica, Chinese Academy of Sciences. *db/db* and *ob/ob* male mice were obtained from the Jackson Laboratory (CA, USA) and were housed in a room maintained at 20–25 °C, 50% relative humidity and a 12-h light/12-h dark cycle with food and water ad libitum. Eight-week-old male mice were divided into three groups by fasting blood glucose and body weight. Vehicle or IVQ-HCl (23, 46 mg/kg) was orally administered by gavage needle daily for 5 weeks ($n = 8$). Fasting blood glucose levels from 6-h fasted mice were measured weekly. For the oral glucose tolerance test (OGTT)/pyruvate tolerance test (PTT), the mice were fasted for 16 h at the fourth/fifth week, and glucose (1.5 g/kg)/pyruvate (1.5 g/kg) was administered orally/intraperitoneally. The glucose levels were measured from tail vein blood samples at 0, 15, 30, 60, 90, and 120 min by ACCU-CHEK (Roche, Basel, Switzerland). At the termination of the assay, the mice were sacrificed, and liver tissues were stored at −80 °C for analysis.

For pharmacokinetic assay in vivo, the mice were administered IVQ-HCl (30 mg/kg, po.; 5 mg/kg, iv.), and rats were administered IVQ-HCl (20 mg/kg, po.; 10 mg/kg, iv.). The plasma samples were then collected to detect the concentrations of IVQ at 0.25, 0.5, 1, 2, 4, 8, and 24 h, finally fitting out the related pharmacokinetic parameters. The metabolite of IVQ was detected and confirmed by standard samples of QVO in mouse plasma after oral administration. The QVO concentration was determined in the liver tissues of the mice and rats at the peak time.

Statistical analysis

All values are presented as the mean ± SEM. Significant differences of two groups were compared by two-tailed unpaired Student's *t*-test, and multiple treatment groups were compared within individual experiments by ANOVA. A P-value < 0.05 was considered to be statistically significant. Significant differences were shown as $^{*}P < 0.05$, $^{**}P < 0.01$, and $^{***}P < 0.001$. Unless otherwise indicated, all experiments were repeated at least three times.

RESULTS

QVO inhibits hepatic gluconeogenesis

QVO inhibits hepatic glucose production: Initially, we found that QVO (Fig. 1a) could inhibit HGP based on the previously reported screening platform [8]. In the assay, sodium lactate (20 mM) and sodium pyruvate (2 mM) were used as gluconeogenic substrates. As indicated in Fig. 1b, QVO (1, 10, 20 μM) efficiently suppressed glucagon-stimulated HGP in primary hepatocytes.

QVO inhibits gluconeogenic rate-limiting enzymes G6Pase and PEPCK: Next, we tested the activity of QVO in suppressing gluconeogenesis by q-PCR to investigate the mRNA levels of the gluconeogenic rate-limiting enzymes glucose-6-phosphatase (G6Pase) and phosphoenolpyruvate carboxykinase (PEPCK) in hepatocytes. Incubation of QVO (1, 10, 20 μM) with glucagon efficiently reduced the mRNA levels of G6Pase and PEPCK compared with the results with glucagon treatment (Fig. 1c, d).

Therefore, these results demonstrated that QVO inhibits hepatic gluconeogenesis.

QVO inhibits hepatic gluconeogenesis involving AMPK

QVO activates AMPK phosphorylation: Next, we investigated the underlying mechanism of QVO in inhibiting gluconeogenesis. As shown in Fig. 2a, Western blotting indicated that treatment with QVO (1, 10, 20 μM) for 4 h dose dependently activated AMPK phosphorylation but had no effects on total AMPK in primary hepatocytes. In addition, the AMPK agonist A-769662 (1 μM, as a positive control) effectively increased the recombinant-AMPK enzyme activity, but QVO (20 μM) had no effects on AMPK enzyme activity (Fig. 2b), suggesting that QVO is an indirect activator of AMPK and activates AMPK phosphorylation.

QVO inhibits hepatic gluconeogenesis partially via AMPK phosphorylation: Because we have determined that QVO inhibited hepatic gluconeogenesis and stimulated AMPK phosphorylation, we next examined whether the inhibition of QVO against hepatic gluconeogenesis was required by its AMPK activation. As shown in Fig. 2c, co-incubation with the AMPK inhibitor compound C (20 μM) for 4 h impeded QVO-induced AMPK phosphorylation in hepatocytes. However, in the HGP assay, we noticed that compound C mildly antagonized the effect of QVO on HGP reduction and the decrease rates of HGP caused by QVO in the absence (18.33%) or presence (15.38%) of compound C were close (Fig. 2d). Next, we conducted q-PCR using AMPK-siRNA. As shown in Fig. 2e and f, AMPK-siRNA obviously antagonized the inhibition of QVO against G6Pase, although QVO still reduced the PEPCK mRNA level.

Because the main downstream target of AMPK related to hepatic gluconeogenesis is the cAMP-responsive element-binding protein-regulated transcription co-activator 2 (TORC2) [13], we detected the effect of QVO on TORC2 phosphorylation at Ser171. As shown in Fig. 2g, QVO (20 μM) and metformin (2 mM, as a positive control) increased the TORC2 phosphorylation level.

These results suggested that QVO might inhibit hepatic gluconeogenesis involving the AMPK pathway.

QVO activates AMPK phosphorylation involving CaMKKβ and LKB1 pathways

QVO activates AMPK phosphorylation involving the CaMKKβ and LKB1 pathways: We next investigated the potential pathways involved in the QVO-induced AMPK activation. Considering that AMPK activity is closely related to the phosphorylation on Thr172 of α subunit by upstream kinases CaMKKβ and LKB1 [14], we wondered whether CaMKKβ or LKB1 signaling participated in the QVO-induced AMPK phosphorylation. As shown in Fig. 3a, QVO-induced AMPK phosphorylation was partially attenuated by the CaMKKβ inhibitor STO609 (2 μg/mL) [15] in hepatocytes. Additionally, STO609 (2 μg/mL) weakened QVO-induced HGP reduction from 12.25% to 8.66% (Fig. 3b) and STO609 antagonized the inhibition of QVO against the G6Pase mRNA level (Fig. 3c). Thus, these results demonstrated that the CaMKKβ pathway is at least involved in the regulation of QVO against AMPK phosphorylation.

To investigate the potential participation of LKB1 signaling in QVO-induced AMPK activation, we carried out the RNA

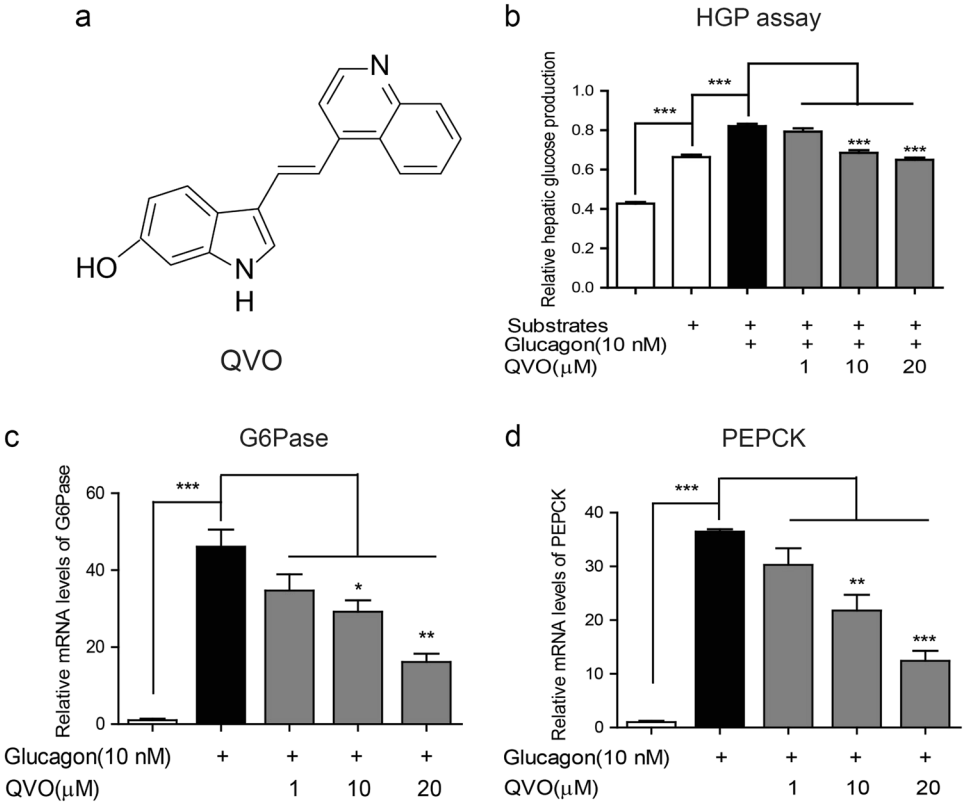

Fig. 1 QVO inhibits hepatic gluconeogenesis. **a** Chemical structure of QVO. **b** QVO (1, 10, 20 μM) inhibited the glucagon-induced HGP in a dose-dependent manner. **c**, **d** Primary hepatocytes were cultured with QVO (1, 10, 20 μM) for 24 h, and then co-incubated with glucagon (10 nM) together for another 2 h, finally harvested for q-PCR assay to determine the mRNA levels of G6Pase (**c**) and PEPCK (**d**). All data were obtained from three independent experiments and presented as mean ± SEM (*$P < 0.05$, **$P < 0.01$, ***$P < 0.001$)

interference assay to knockdown LKB1 in primary hepatocytes as described previously [9]. As demonstrated in Fig. 3e, LKB1 knockdown efficiently reduced QVO-induced AMPK phosphorylation, suggesting that LKB1 signaling was also involved in the regulation of QVO against AMPK phosphorylation. Moreover, we conducted q-PCR in hepatocytes transfected with LKB1-siRNA. As shown in Fig. 3f and g, LKB1-siRNA at least partially blocked the inhibition effect of QVO on gluconeogenesis genes. STO609 and LKB1-siRNA together completely revised the stimulation of QVO on AMPK phosphorylation (Fig. 3h).

Taken together, these results indicated that the two upstream signals CaMKKβ and LKB1 are involved in the regulation of QVO against AMPK and gluconeogenesis.

QVO inhibits the mitochondrial function-related signaling pathway

QVO inhibits mitochondrial function: To date, the suppression of AMPK activation against hepatic gluconeogenesis is under much debate. An increasing number of reports have indicated that AMPK is not probably requisite for hepatic gluconeogenesis regulation in related genetic loss-of-function studies [16, 17]. For example, metformin inhibits hepatic gluconeogenesis in an LKB1- and AMPK-independent manner via a decrease in the hepatic energy state involving decreasing ATP level [18]. Therefore, we next detected the influence of QVO on the ATP level. The results in Fig. 4a showed that QVO (1, 10, 20 μM) decreased the ATP content in a dose-dependent manner. Given that ATP is primarily generated in mitochondria and a decrease in the mitochondrial membrane potential ($\Delta\Psi_m$) is accompanied by reduced ATP production [19], we evaluated the influence of QVO on $\Delta\Psi_m$. As indicated in Fig. 4b, QVO (1, 10, 20 μM) could reduce $\Delta\Psi_m$ with 4-h treatment, and QVO (20 μM) decreased ΔΨm in a relatively mild manner compared with CCCP (10 μM, a positive control) [19] in primary hepatocytes. In addition, the MTT assay (Fig. 4c) revealed that QVO (1, 10, 20 μM) rendered no effects on cell viability in primary hepatocytes. These results indicated that QVO inhibits mitochondrial function without inducing cell toxicity.

QVO inhibits the activities of mitochondrial respiratory complexes I and III: To determine whether ATP reduction was implicated in cellular mitochondrial respiration, we examined oxygen consumption in primary hepatocytes and found that QVO (1, 10, 20 μM) dose dependently inhibited respiration (Fig. 4d). Reports have indicated that the activation of AMPK leads to enhanced mitochondrial biogenesis [20] and mitochondrial function inhibition-induced energy reduction, in turn, is an upstream signal to activate AMPK [21]. However, a recent report showed that the mitochondrial respiratory chain complex I inhibitor rotenone induced glycolysis and reduced hepatic glucose output via a non-AMPK pathway, although rotenone also activated AMPK [22]. Thus, we assessed the potential effects of QVO on mitochondrial respiratory complexes. In the assay, the primary hepatocytes were incubated with QVO (20 μM) or the corresponding positive compounds (metformin vs. complex I, phenformin vs. complex II [23], antimycin A vs. complex III [24], phenformin vs. complex IV [23], oligomycin vs. complex V [24]) for 4 h, and mitochondria were isolated to determine the activity of respiratory complexes. As shown in Fig. 4e, QVO (20 μM) inhibited the activities of mitochondrial respiratory complexes I and III instead of those of complex II, IV or V.

These results thus implied that QVO inhibits the mitochondrial function-related signaling pathway.

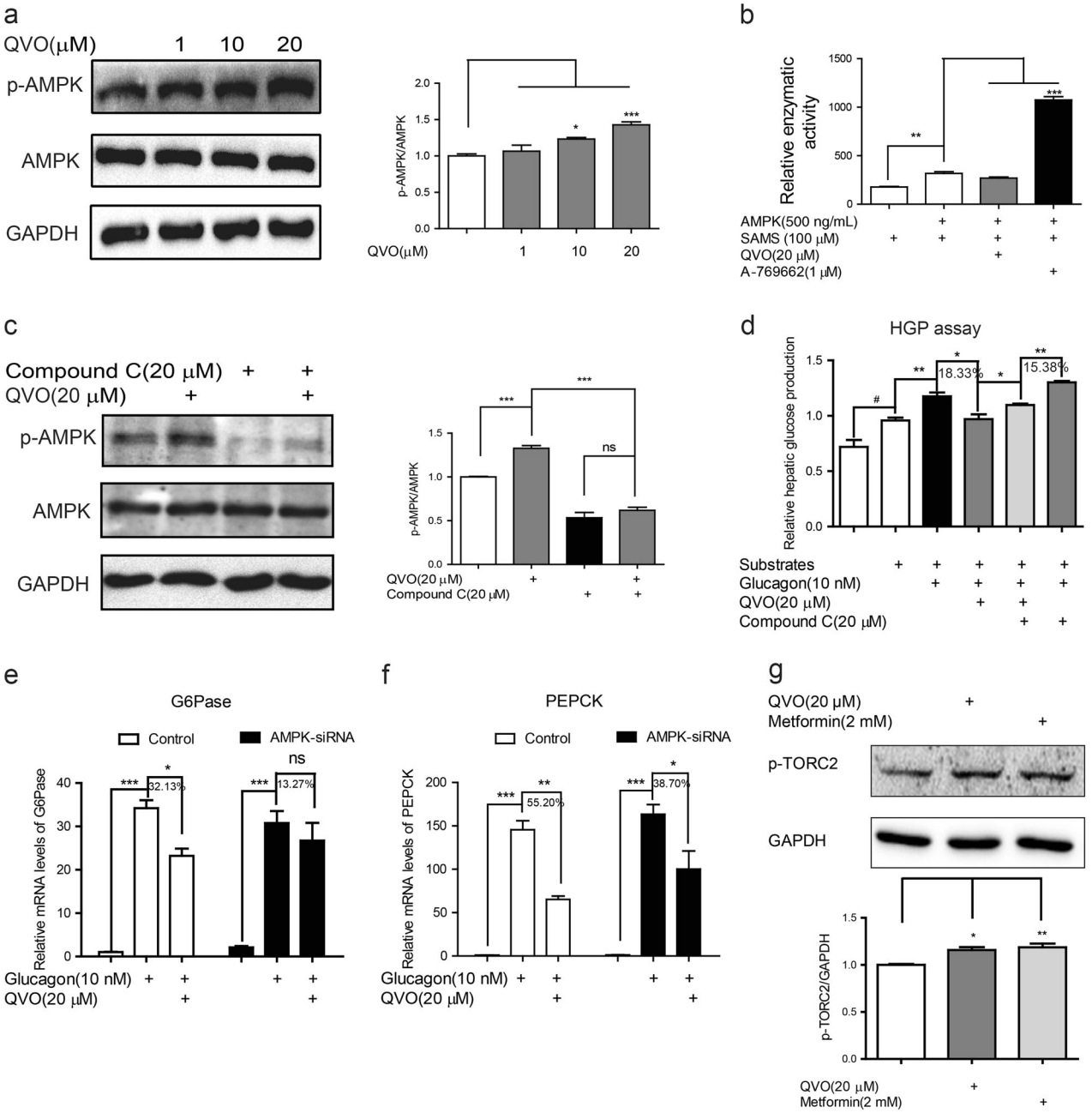

Fig. 2 QVO inhibits hepatic gluconeogenesis involving AMPK activation. **a** Primary hepatocytes were cultured with QVO (1, 10, 20 μM) for 4 h, and then collected for Western blot assay with antibodies against p-AMPK and AMPK. **b** A-769662 (1 μM), as a positive control, increased the activity of recombinant AMPK enzyme. QVO (20 μM) exhibited no influence on the recombinant AMPK activity. **c** Primary hepatocytes were cultured with QVO (20 μM) with or without compound C (20 μM) for 4 h, and then collected for Western blot assay with antibodies against p-AMPK and AMPK. **d** Compound C (20 μM) involved HGP assay was conducted. **e**, **f** AMPK-siRNA (100 pM)-transfected primary hepatocytes were cultured with QVO (20 μM) for 24 h, and then co-incubated with glucagon (10 nM) together for another 2 h, finally harvested for q-PCR assay to determine the mRNA levels of G6Pase (**e**) and PEPCK (**f**). **g** Primary hepatocytes were cultured with QVO (20 μM) and metformin (2 mM) for 4 h, and then collected for Western blot assay with antibodies against p-TORC2. All data were obtained from three independent experiments and presented as mean ± SEM (*$P < 0.05$, **$P < 0.01$, ***$P < 0.001$; ns, no significance)

IVQ, as a prodrug of QVO, efficiently ameliorates hyperglycemia in *db/db* and *ob/ob* mice

IVQ functions as a prodrug of QVO: To evaluate the activity of QVO in anti-T2DM in vivo, we synthesized an increased amount of QVO for animal experiments. Given the complicated synthesis route and low yield of QVO (Fig. 5a) and that the hydroxylation pathway is a principal metabolic pathway associated with cytochrome P450 enzymes (CYPs) activation [25, 26], we next carried out the relevant prodrug design and speculated that IVQ, as a potential prodrug with easier synthesis route and higher yield (Fig. 5b), could be converted into QVO after metabolic reaction (Fig. 5c). Accordingly, we performed the related pharmacokinetic assay in vivo. To improve the solubility of IVQ, IVQ-HCl was administered instead of IVQ in vivo [27]. The results demonstrated that IVQ was

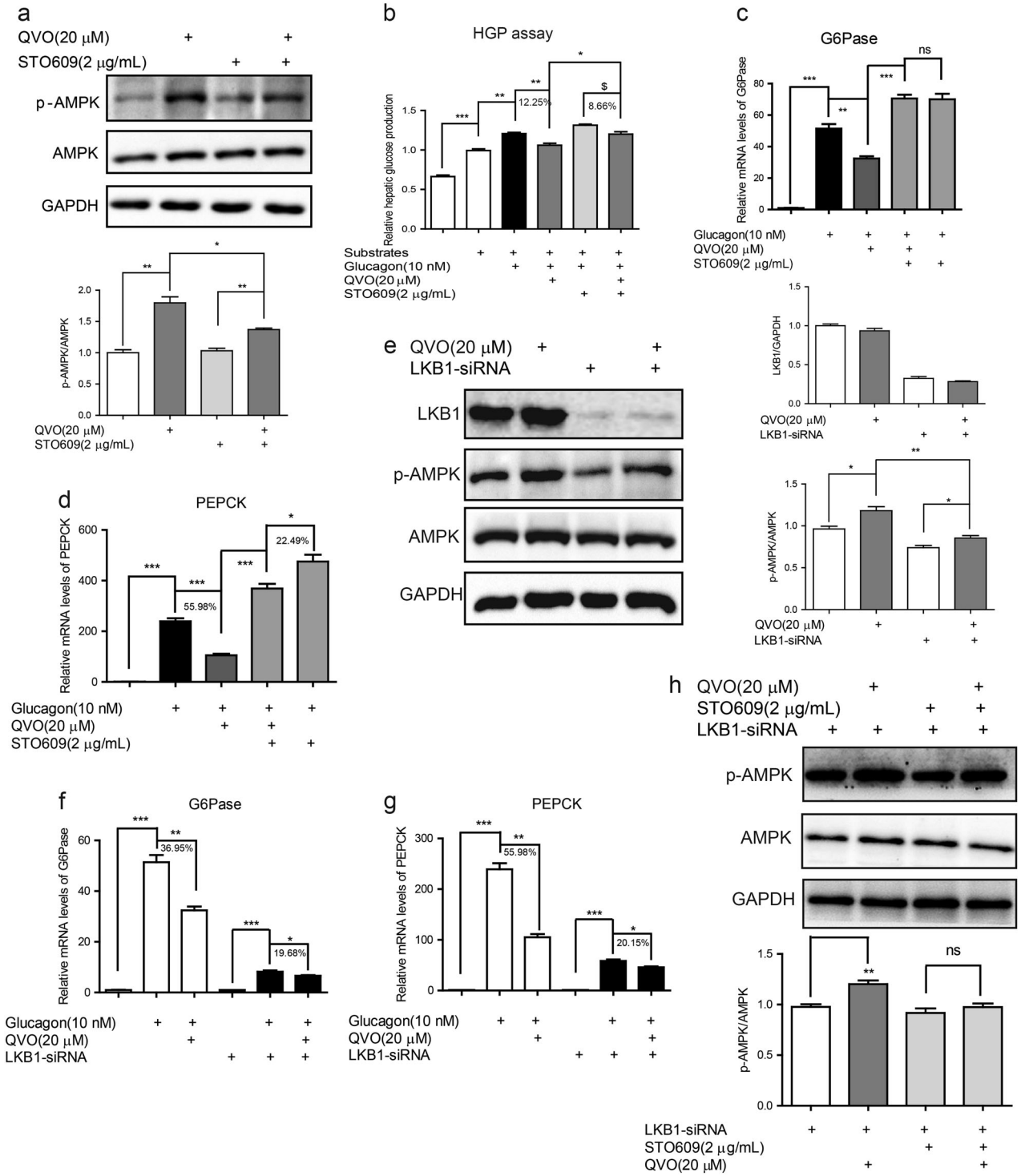

Fig. 3 QVO activates AMPK phosphorylation involving CaMKKβ and LKB1 pathways. **a** Primary hepatocytes were cultured by QVO (20 μM) with or without CaMKKβ inhibitor STO609 (2 μg/mL) for 4 h, and then collected for Western blot assay with antibodies against p-AMPK and AMPK. **b** STO609 (2 μg/mL) involved HGP assay was conducted. **c**, **d** STO609 (2 μg/mL) involved q-PCR assay was conducted. **e** Primary hepatocytes were transfected with LKB1-siRNA (100 pM) for 24 h, and then treated with QVO (20 μM) for 4 h, finally collected for Western blot assay with antibodies against LKB1, p-AMPK, and AMPK. **f**, **g** AMPK-siRNA (100 pM)-transfected primary hepatocytes were cultured with QVO (20 μM) for 24 h, and then co-incubated with glucagon (10 nM) together for another 2 h, finally harvested for q-PCR assay to determine the mRNA levels of G6Pase (**f**) and PEPCK (**g**). **h** LKB1-siRNA (100 pM)-transfected primary hepatocytes were treated with QVO (20 μM) and STO609 (2 μg/mL) for 4 h, finally collected for Western blot assay with antibodies against p-AMPK and AMPK. All data were obtained from three independent experiments and presented as mean ± SEM (*$P < 0.05$, **$P < 0.01$, ***$P < 0.001$, ns, no significance)

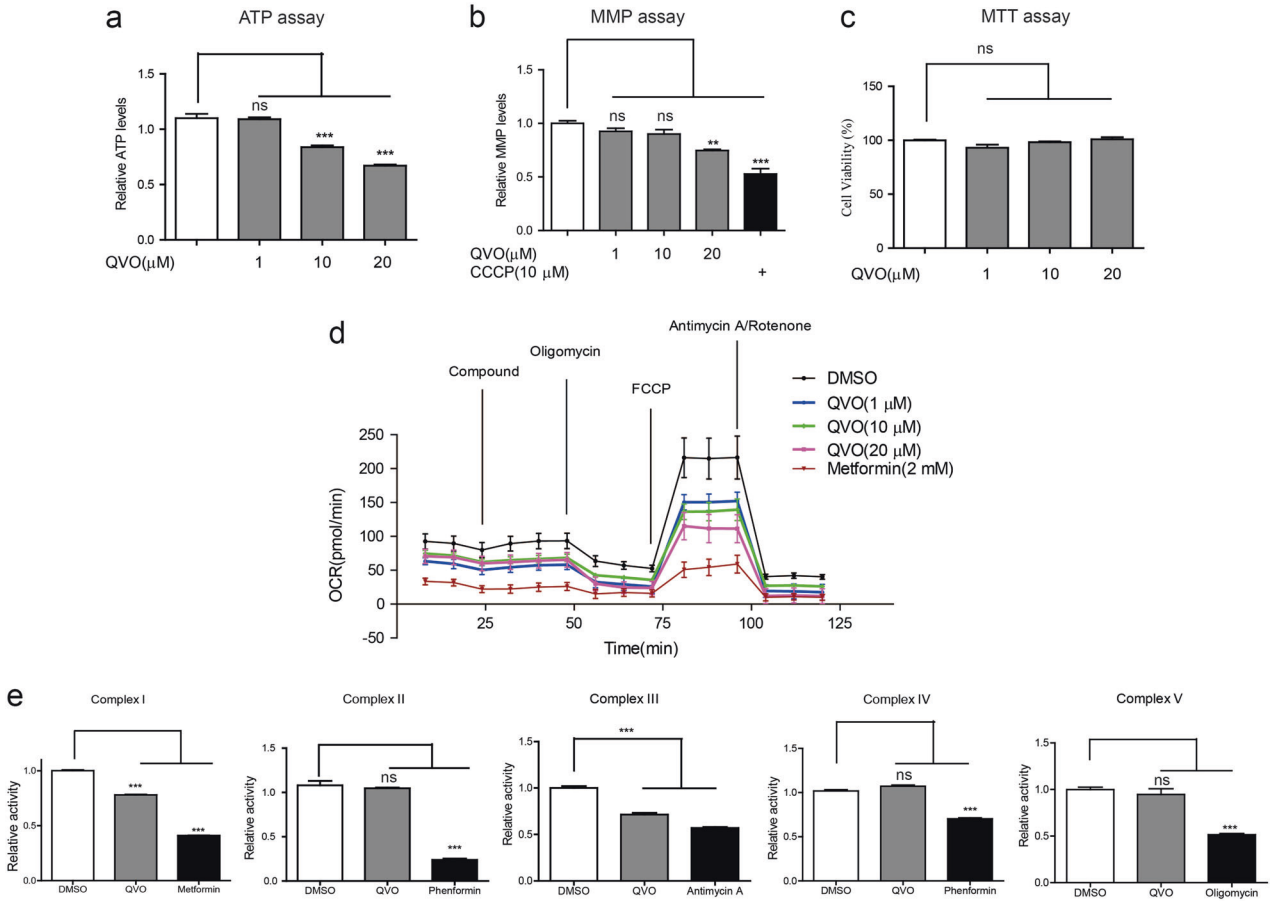

Fig. 4 QVO inhibits mitochondrial function-related signaling pathway. **a** Primary hepatocytes were treated with QVO (1, 10, 20 μM) for 4 h, and then ATP content was detected. **b** Primary hepatocytes were treated with QVO (1, 10, 20 μM) or CCCP (10 μM, a positive control) for 4 h, and then $\Delta\Psi_m$ values were detected. **c** Primary hepatocytes were treated with QVO (1, 10, 20 μM) for 24 h, and then used for MTT assay to detect cell viability. **d** Primary hepatocytes were treated with QVO (1, 10, 20 μM) or metformin (as a positive control) for 4 h, and then oxygen consumption of respiration was detected according to Seahorse XF cell mito stress test kit on Seahorse XFe96. **e** Primary hepatocytes were treated with QVO (20 μM) or corresponding positive controls (metformin vs. complex I, phenformin vs. complex II, antimycin A vs. complex III, phenformin vs. complex IV, oligomycin vs. complex V) for 4 h, and collected for mitochondria isolation to detect the activity of mitochondrial respiratory complexes. All data were obtained from three independent experiments and presented as mean ± SEM (**$P < 0.01$, ***$P < 0.001$, ns, no significance)

quickly metabolized with a short half-life in mice and rats (Table 1). We also found that IVQ itself could not reduce the HGP stimulated by glucagon (Fig. 5d). In addition, QVO was the main metabolite of IVQ in mice orally administered IVQ-HCl (Fig. 5e). We also determined that IVQ could be converted to QVO in mice and rats (Supplemental Table 1), and the half-life of QVO was longer than that of IVQ (Supplemental Table 2). In addition, the QVO concentration reached 129.84 ± 15.42 and 281.30 ± 54.87 ng/g (mean ± SEM, $n = 3$) in the liver tissues of mice and rats at the peak time of QVO. These results indicated that IVQ functions as a prodrug of QVO.

IVQ ameliorates hyperglycemia in db/db and ob/ob mice: Because QVO has been found to be capable of inhibiting hepatic gluconeogenesis in hepatocytes, we next examined the capability of its prodrug IVQ in ameliorating hyperglycemia against T2DM model mice. It was found that IVQ-HCl administration obviously decreased the fasting blood glucose and HbA1c levels (Fig. 6a, b) and improved the glucose (Fig. 6c, d) and pyruvate tolerance (Fig. 6e, f) in both model mice. Therefore, all results demonstrated that IVQ ameliorates hyperglycemia in *db/db* and *ob/ob* mice.

Taken together, these above results suggested that IVQ, as a prodrug of QVO, efficiently ameliorates hyperglycemia in *db/db* and *ob/ob* mice.

IVQ suppresses hepatic gluconeogenesis and activates the AMPK signaling pathway in *db/db* and *ob/ob* mice

IVQ suppresses hepatic gluconeogenesis in db/db and ob/ob mice: Given that IVQ improved pyruvate tolerance in vivo, we further assessed its capability in suppressing gluconeogenesis in the liver tissues of *db/db* and *ob/ob* mice. In addition, as shown in Fig. 7a–d, IVQ-HCl treatment reduced the mRNA levels of G6Pase and PEPCK in either of the model mice, indicating that IVQ suppresses hepatic gluconeogenesis in *db/db* and *ob/ob* mice.

IVQ activates the AMPK pathway in db/db and ob/ob mice: Next, we also evaluated the potential of IVQ in regulating the AMPK signaling pathway in the liver tissues of *db/db* and *ob/ob* mice. As indicated in Fig. 7e and f, IVQ-HCl treatment increased the phosphorylation level of AMPK in the liver tissues of either model mice, thereby suggesting that IVQ activates the AMPK pathway in *db/db* and *ob/ob* mice.

Thus, all above results suggested that IVQ suppresses hepatic gluconeogenesis and activates AMPK phosphorylation in *db/db* and *ob/ob* mice.

IVQ exhibits no apparent serum-related toxicity in *db/db* and *ob/ob* mice

Given the highly anti-diabetic activity of IVQ, we also detected serum-related toxicity in *db/db* and *ob/ob* mice. The results

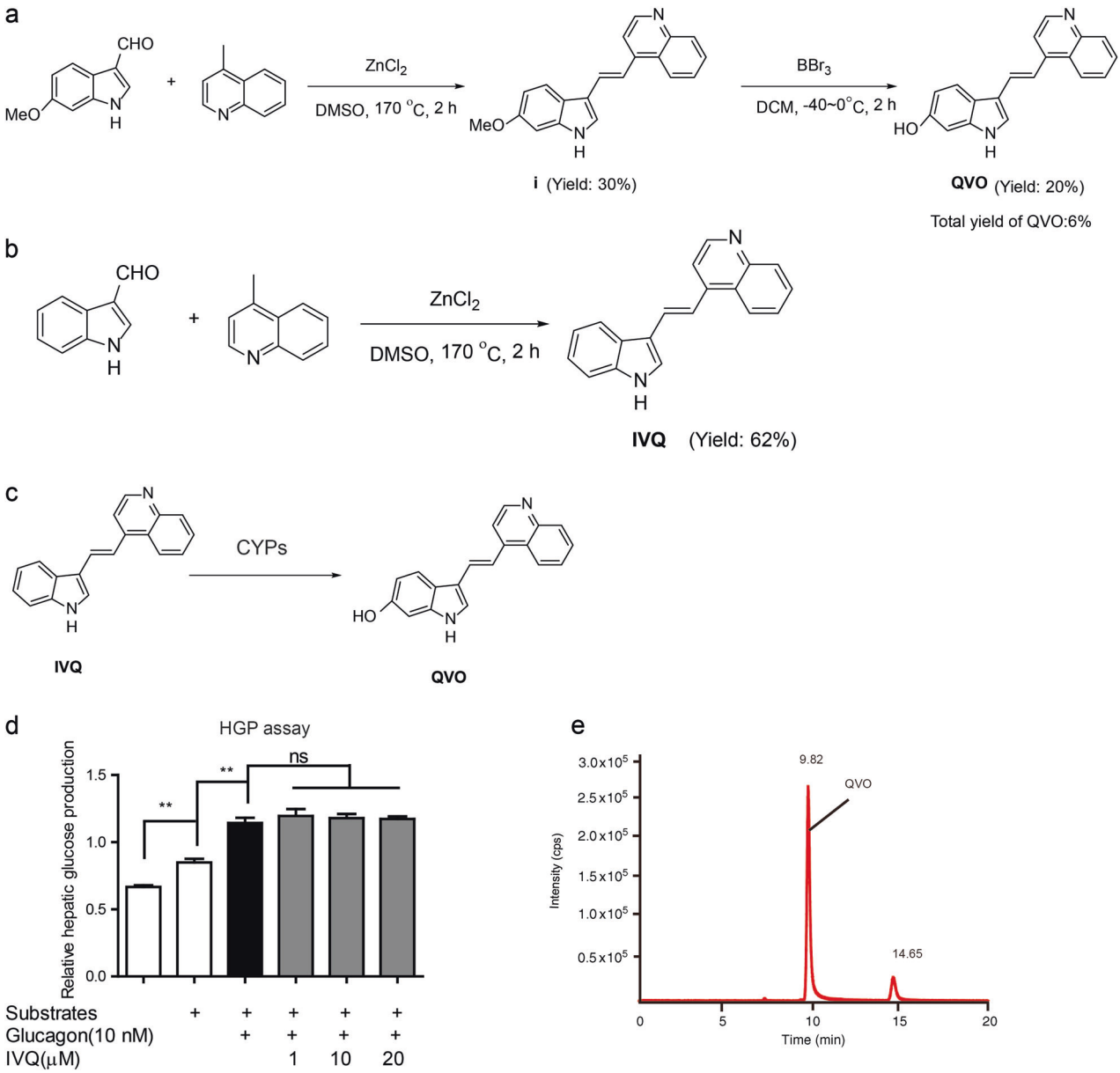

Fig. 5 The prodrug design of QVO based on CYPs system. **a** Synthetic route of QVO. **b** Synthetic route of IVQ. **c** Prodrug design of QVO based on CYPs system. **d** IVQ involved HGP assay was conducted. The data were obtained from three independent experiments and presented as mean ± SEM (**$P < 0.01$, ns, no significance). **e** QVO was the main metabolite of IVQ in mice orally administered with IVQ (30 mg/kg, $n = 3$) after 15 min

indicated that IVQ-HCl treatment failed to influence the serum alanine aminotransferase (ALT, Supplemental Fig. 1a), aspartate aminotransferase (AST, Supplemental Fig. 1b), albumin (ALB, Supplemental Fig. 1c), total bilirubin (TB, Supplemental Fig. 1d), or total protein (TP, Supplemental Fig. 1e) levels in both model mice, demonstrating that the administration of IVQ (23, 46 mg/kg every day) for 5 weeks exhibits no apparent serum-related toxicity in T2DM model mice.

IVQ exhibits no apparent cardiovascular system dysfunction or genotoxicity

Because adverse effects on the cardiovascular system and genotoxicity are the main causes of failure in the development of new drugs [28, 29], we preliminarily assessed the effect of IVQ on cardiovascular system function in beagle dogs and genotoxicity on *Salmonella typhimurium* strains using the electrocardiogram and ames assays. The electrocardiogram assay indicated that the single-dose oral treatment of IVQ-HCl (10, 30, 100 mg/kg) exerted no changes in arrhythmia or drug-correlated changes in electrocardiogram validation marks, including the heart rate, RR interval, PR interval, QRS duration, and QT interval within 24 h (Supplemental Table 3), and the ames assay showed that there were no significant differences in the revertant colony numbers between IVQ (1–1000 μg/plate) and the negative control in *Salmonella typhimurium* strains TA98 and TA100 (Supplemental Table 4). These results demonstrated that IVQ exhibits no apparent cardiovascular system dysfunction or genotoxicity.

Table 1. Pharmacokinetic assay of IVQ-HCl in mice and rats by intravenous injection (iv.) or oral administration (po.)

	Mice (mean ± SEM)		Rats (mean ± SEM)	
Parameters	iv.(5 mg/kg)	*po.*(30 mg/kg)	iv.(10 mg/kg)	*po.*(20 mg/kg)
$AUC_{(0-t)}$ (ng/mL*h)	1735.3 ± 32.2	5420 ± 1893.9	8358.4 ± 943.4	3942.6 ± 201.4
$AUC_{(0-\infty)}$ (ng/mL*h)	1740.6 ± 30.4	6535.5 ± 962.2	8394.3 ± 937.4	3957.6 ± 211.4
$MRT_{(0-t)}$ (h)	0.58 ± 0.2	9.71 ± 3.5	1.19 ± 0.1	3.58 ± 0.6
V_Z (L/kg)	10.63 ± 9.1	138 ± 123.6	1.61 ± 0.1	18.87 ± 2.2
CL_Z (L/h/kg)	2.87 ± 0.1	4.78 ± 0.6	1.22 ± 0.1	5.08 ± 0.3
$T_{1/2Z}$ (h)	2.54 ± 2.2	2.47 ± 1.7	0.94 ± 0.1	2.62 ± 0.4
T_{max} (h)	—	0.5 ± 0.2	—	0.25 ± 0
C_{max} (ng/mL)	4100.2 ± 471.5	1078.9 ± 298.6	8151.7 ± 325.2	1812.3 ± 116.3
F%	—	52.1 ± 18.2	—	23.6 ± 1.2

The dosages for mice were 5 mg/kg (iv.) and 30 mg/kg (*po.*), and for rats were 10 mg/kg (iv.) and 20 mg/kg (*po.*). Data were shown as mean ± SEM, $n = 3$

DISCUSSION

The liver, as one of the major organs responsible for glucose metabolism regulation, is closely related to T2DM, metabolic syndrome and fatty liver [30]. Suppressing excessive hepatic gluconeogenesis is believed to be an ideal strategy to reduce blood glucose [31]. In the current study, we screened laboratory in-house compounds and discovered that the small-molecule compound QVO, as a gluconeogenesis inhibitor, effectively suppressed HGP. Mechanistic studies demonstrated that QVO activated the CaMKKβ- and LKB1-AMPK pathways and inhibited the mitochondrial function pathway. IVQ, as a prodrug of QVO, patently ameliorated glucose homeostasis in T2DM model mice. The successful findings of QVO and its prodrug IVQ in suppressing hepatic gluconeogenesis and ameliorating glucose homeostasis have confirmed that targeting gluconeogenesis inhibition should be a promising strategy for T2DM treatment. Our work has also highlighted the potential druggability of IVQ in the treatment of T2DM.

AMPK is widely expressed in mammalian tissues, plays an important role in controlling energy homeostasis and glucose

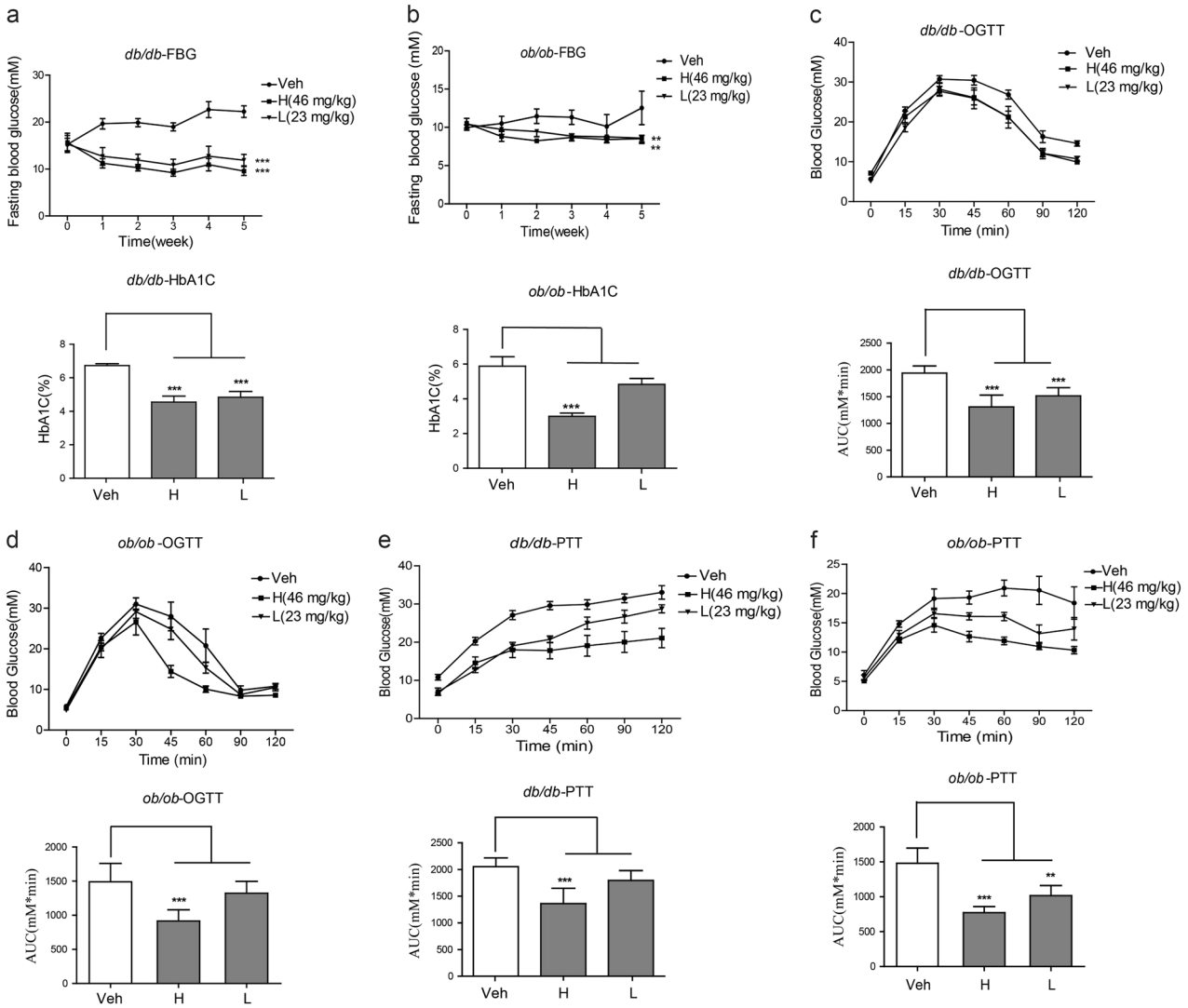

Fig. 6 IVQ efficiently ameliorates hyperglycemia in *db/db* and *ob/ob* mice. **a**, **b** Fasting blood glucose and HbA1c levels were detected in *db/db* mice (**a**) and *ob/ob* mice (**b**) with treatment of IVQ-HCl (23, 46 mg/kg every day) ($n = 8$). **c**, **d** OGTT assay was performed in *db/db* mice (**c**) and *ob/ob* mice (**d**) after treatment with IVQ-HCl (23, 46 mg/kg every day) for 4 weeks ($n = 8$). **e**, **f** PTT assay was performed in *db/db* mice (**e**) and *ob/ob* mice (**f**) after treatment with IVQ-HCl (23, 46 mg/kg every day) for 5 weeks ($n = 8$). Veh: vehicle; H: 46 mg/kg; L: 23 mg/kg. All data were presented as mean ± SEM (**$P < 0.01$, ***$P < 0.001$)

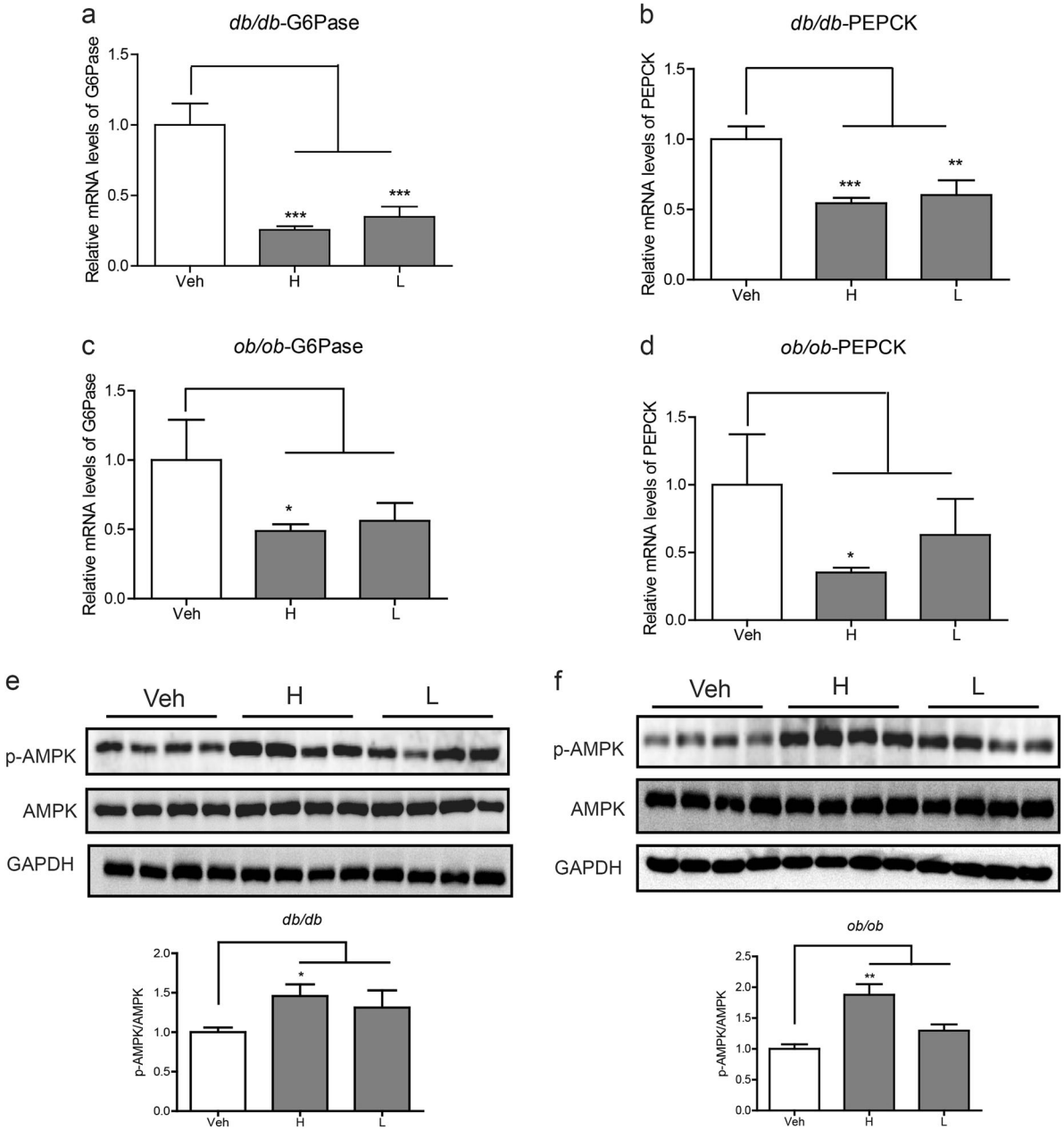

Fig. 7 IVQ inhibits hepatic gluconeogenesis and activates AMPK in *db/db* and *ob/ob* mice. **a**–**d** Liver tissues of *db/db* and *ob/ob* with treatment of IVQ-HCl (23, 46 mg/kg every day) for 5 weeks were used for q-PCR assay to detect the mRNA levels of G6Pase and PEPCK ($n = 8$). **e**, **f** Liver tissues of *db/db* mice (**e**) or *ob/ob* (**f**) mice with treatment of IVQ-HCl (23, 46 mg/kg every day) for 5 weeks were used for Western blot assay with antibodies against p-AMPK and AMPK ($n = 4$). Veh: vehicle; H: 46 mg/kg; L: 23 mg/kg. All data were presented as mean ± SEM (*$P < 0.05$, **$P < 0.01$, ***$P < 0.001$)

metabolism, and has become an attractive potential therapeutic target for many diseases, including diabetes, cancer, heart disease, viral infection, and inflammatory disorders [32], although there are no AMPK direct activators in clinical use due to the poor pharmacokinetic profiles or off-target effects of the agents [33, 34]. Thus, further study on AMPK regulation might help to expound new activation mechanisms or develop compounds with better pharmacokinetic profiles [33].

AMPK activity can be directly regulated by binding AMP to the regulatory γ subunit or indirectly by phosphorylation on Thr172 of the α subunit by upstream kinases [5]. It is reported that binding AMP to the γ subunit greatly stimulates LKB1-dependent AMPKα phosphorylation on Thr172, and AMP binding inhibits dephosphorylation through protein phosphatases, such as PP2A and PP2C [35]. The downstream targets of AMPK include acetyl-CoA carboxylase related to fatty acids oxidation [33]; tuberous sclerosis complex 2 related to mammalian target of rapamycin complex 1 and protein synthesis [36]; 3-hydroxy-3-methylglutaryl-coenzyme A reductase related to cholesterol synthesis [37]; peroxisome proliferator-activated receptor-gamma co-activator 1α related to mitochondrial biogenesis [38] and TORC2 related to hepatic gluconeogenesis [13]. However, the AMPK-independent mechanism of hepatic gluconeogenesis suppression by metformin suggests the dispensability of AMPK in hepatic gluconeogenesis [39]. It is highlighted that metformin inhibits hepatic gluconeogenesis in an LKB1- and AMPK-independent manner via a decrease in the hepatic

energy state involving decreasing ATP levels through the inhibition of complex I [18]. Moreover, moderate inhibition against mitochondrial function is believed to be beneficial to anti-diabetes [19], and inhibition of mitochondrial complex I stimulates glucose consumption and decreases HGP independently of AMPK activation [22]. To date, both AMPK-dependent and AMPK-independent mechanisms of metformin for hepatic gluconeogenesis inhibition have been determined, a key factor is the dosage of metformin used [39]. A potential explanation for this discrepancy may be that AMP might have an additional AMPK-independent effect, lowering cAMP and reducing the expression of gluconeogenic enzymes [40]. Herein, the small molecule QVO, as an indirect AMPK activator, activated AMPK phosphorylation and reduced the ATP level, indicating that QVO might suppress hepatic gluconeogenesis via AMPK-dependent and -independent mechanisms. The precise underlying mechanism of QVO in AMPK and mitochondrial respiratory chain remains to be investigated. Additionally, QVO, as an AMPK activator, might have more potential in drug discovery against metabolic diseases.

CYPs are important biological enzymes in the body with many molecules as substrates for enzymatic reactions [41]. They are major enzymes involved in drug metabolism, accounting for approximately 75% of the total metabolism [42] and the hydroxylation pathway is a primary metabolic pathway related to CYPs activation [26]. The current study suggested that QVO, as a main metabolite of IVQ, functioned in hepatic gluconeogenesis inhibition, although more studies related to QVO are needed. Our results have implied the potential of CYPs in drug design—for example, by using different CYPs to achieve targeted drug delivery, design prodrugs, promote efficacy or decrease the adverse effects of drugs [43].

In conclusion, the small molecule QVO probably suppressed hepatic gluconeogenesis involving CaMKKβ- and LKB1-AMPK pathways and mitochondrial function-related signaling pathway. IVQ, designed as a prodrug of QVO, efficiently ameliorated glucose homeostasis in *db/db* and *ob/ob* mice without obvious cardiovascular system dysfunction or genotoxicity. Our current work has addressed the advantage of CYPs in drug design and potential of IVQ in the treatment of T2DM.

ACKNOWLEDGEMENTS

This work was supported by the National Natural Science Foundation of China (Grant numbers 81473141, 81703806, 81800430), NSFC-TRF collaboration projects (Grant numbers NSFC 81561148011), the Priority Academic Program Development of Jiangsu Higher Education Institutions (Integration of Chinese and Western Medicine), the Fundamental Research Funds for the Central Universities (Grant number JUSRP11863), and Project funded by China Postdoctoral Science Foundation (Grant number 2018M642172).

AUTHOR CONTRIBUTIONS

XS, JC, and TTZ were responsible for the conception and design of the study. TTZ, TZ, YR, QYY, and GHW designed and performed experiments. FM, YNZ, JJ, and LHH contributed to the acquisition of IVQ-HCl. TTZ and XS were responsible for drafting the manuscript. JR, XWG, JG, YHZ, and JMY gave advice on the manuscript preparation. XS is the guarantor of this work and, as such, has full access to all the data in the study and takes responsibility for the integrity of the data and accuracy of the data analysis. All authors approved the manuscript.

ADDITIONAL INFORMATION

The online version of this article (https://doi.org/10.1038/s41401-018-0208-2) contains supplementary material, which is available to authorized users.

Competing interests: The authors declare no competing interests.

REFERENCES

1. Lemes Dos Santos PF, Dos Santos PR, Ferrari GS, Fonseca GA, Ferrari CK. Knowledge of diabetes mellitus: does gender make a difference? Osong Public Health Res Perspect. 2014;5:199–203.
2. An H, He L. Current understanding of metformin effect on the control of hyperglycemia in diabetes. J Endocrinol. 2016;228:R97–106.
3. Rui L. Energy metabolism in the liver. Compr Physiol. 2014;4:177–97.
4. Weikel KA, Ruderman NB, Cacicedo JM. Unraveling the actions of AMP-activated protein kinase in metabolic diseases: systemic to molecular insights. Metabolism. 2016;65:634–45.
5. Ramesh M, Vepuri SB, Oosthuizen F, Soliman ME. Adenosine monophosphate-activated protein kinase (AMPK) as a diverse therapeutic target: a computational perspective. Appl Biochem Biotechnol. 2016;178:810–30.
6. Yao F, Zhang M, Chen L. Adipose tissue-specialized immunologic features might be the potential therapeutic target of prospective medicines for obesity. J Diabetes Res. 2017;2017:4504612.
7. Ewart MA, Kennedy S. Diabetic cardiovascular disease—AMP-activated protein kinase (AMPK) as a therapeutic target. Cardiovasc Hematol Agents Med Chem. 2012;10:190–211.
8. Zhou TT, Ma F, Shi XF, Xu X, Du T, Guo XD, et al. DMT efficiently inhibits hepatic gluconeogenesis involving Galphaq signaling pathway. J Mol Endocrinol. 2017;59:151–69.
9. Tang X, Zhuang J, Chen J, Yu L, Hu L, Jiang H, et al. Arctigenin efficiently enhanced sedentary mice treadmill endurance. PLoS One. 2011;6:e24224.
10. Zhou TT, Quan LL, Chen LP, Du T, Sun KX, Zhang JC, et al. SP6616 as a new Kv2.1 channel inhibitor efficiently promotes beta-cell survival involving both PKC/Erk1/2 and CaM/PI3K/Akt signaling pathways. Cell Death Dis. 2016;7:e2216.
11. Guo XD, Sun GL, Zhou TT, Wang YY, Xu X, Shi XF, et al. LX2343 alleviates cognitive impairments in AD model rats by inhibiting oxidative stress-induced neuronal apoptosis and tauopathy. Acta Pharmacol Sin. 2017;38:1104–19.
12. Lopez-Fabuel I, Le Douce J, Logan A, James AM, Bonvento G, Murphy MP, et al. Complex I assembly into supercomplexes determines differential mitochondrial ROS production in neurons and astrocytes. Proc Natl Acad Sci U S A. 2016;113:13063–8.
13. Jiang SJ, Dong H, Li JB, Xu LJ, Zou X, Wang KF, et al. Berberine inhibits hepatic gluconeogenesis via the LKB1-AMPK-TORC2 signaling pathway in streptozotocin-induced diabetic rats. World J Gastroenterol. 2015;21:7777–85.
14. Wang G, Xu X, Yao X, Zhu Z, Yu L, Chen L, et al. Latanoprost effectively ameliorates glucose and lipid disorders in *db/db* and *ob/ob* mice. Diabetologia. 2013;56:2702–12.
15. Pyla R, Osman I, Pichavaram P, Hansen P, Segar L. Metformin exaggerates phenylephrine-induced AMPK phosphorylation independent of CaMKKbeta and attenuates contractile response in endothelium-denuded rat aorta. Biochem Pharmacol. 2014;92:266–79.
16. Rena G, Pearson ER, Sakamoto K. Molecular mechanism of action of metformin: old or new insights? Diabetologia. 2013;56:1898–906.
17. Cameron AR, Logie L, Patel K, Bacon S, Forteath C, Harthill J, et al. Investigation of salicylate hepatic responses in comparison with chemical analogues of the drug. Biochim Biophys Acta. 2016;1862:1412–22.
18. Foretz M, Hebrard S, Leclerc J, Zarrinpashneh E, Soty M, Mithieux G, et al. Metformin inhibits hepatic gluconeogenesis in mice independently of the LKB1/AMPK pathway via a decrease in hepatic energy state. J Clin Invest. 2010;120:2355–69.
19. Qiu BY, Turner N, Li YY, Gu M, Huang MW, Wu F, et al. High-throughput assay for modulators of mitochondrial membrane potential identifies a novel compound with beneficial effects on *db/db* mice. Diabetes. 2010;59:256–65.
20. O'Neill HM, Maarbjerg SJ, Crane JD, Jeppesen J, Jorgensen SB, Schertzer JD, et al. AMP-activated protein kinase (AMPK) beta1beta2 muscle null mice reveal an essential role for AMPK in maintaining mitochondrial content and glucose uptake during exercise. Proc Natl Acad Sci U S A. 2011;108:16092–7.
21. Lin SC, Hardie DG. AMPK: sensing glucose as well as cellular energy status. Cell Metab. 2018;27:299–313.
22. Hou WL, Yin J, Alimujiang M, Yu XY, Ai LG, Bao YQ, et al. Inhibition of mitochondrial complex I improves glucose metabolism independently of AMPK activation. J Cell Mol Med. 2018;22:1316–28.
23. Drahota Z, Palenickova E, Endlicher R, Milerova M, Brejchova J, Vosahlikova M, et al. Biguanides inhibit complex I, II and IV of rat liver mitochondria and modify their functional properties. Physiol Res. 2014;63:1–11.
24. Choi EM, Lee YS. Mitochondrial defects and cytotoxicity by antimycin A on cultured osteoblastic MC3T3-E1 cells. Food Chem Toxicol. 2011;49:2459–63.
25. Bojic M, Sedgeman CA, Nagy LD, Guengerich FP. Aromatic hydroxylation of salicylic acid and aspirin by human cytochromes P450. Eur J Pharm Sci. 2015;73:49–56.
26. Tekes K, Kalasz H, Hasan MY, Adeghate E, Darvas F, Ram N, et al. Aliphatic and aromatic oxidations, epoxidation and S-oxidation of prodrugs that yield active drug metabolites. Curr Med Chem. 2011;18:4885–900.
27. Thakuria R, Delori A, Jones W, Lipert MP, Roy L, Rodriguez-Hornedo N. Pharmaceutical cocrystals and poorly soluble drugs. Int J Pharm. 2013;453:101–25.

28. Xing G, Lu J, Hu M, Wang S, Zhao L, Zheng W, et al. Effects of group housing on ECG assessment in conscious cynomolgus monkeys. J Pharmacol Toxicol Methods. 2015;75:44–51.
29. Luo Q, Li Y, Zhang Z. A systematic assessment of genotoxicity on pivaloylacylation-7ADCA-a wide existing antibiotic impurity. Int J Clin Exp Med. 2014;7:4260–71.
30. Kuang JR, Zhang ZH, Leng WL, Lei XT, Liang ZW. Dapper1 attenuates hepatic gluconeogenesis and lipogenesis by activating PI3K/Akt signaling. Mol Cell Endocrinol. 2017;447:106–15.
31. Zheng J, Woo SL, Hu X, Botchlett R, Chen L, Huo Y, et al. Metformin and metabolic diseases: a focus on hepatic aspects. Front Med. 2015;9:173–86.
32. Grahame Hardie D. AMP-activated protein kinase: a key regulator of energy balance with many roles in human disease. J Int Med. 2014;276:543–59.
33. Coughlan KA, Valentine RJ, Ruderman NB, Saha AK. AMPK activation: a therapeutic target for type 2 diabetes? Diabetes Metab Syndr Obes. 2014; 7:241–53.
34. Olivier S, Foretz M, Viollet B. Promise and challenges for direct small molecule AMPK activators. Biochem Pharmacol. 2018;153:147–58.
35. Kim J, Yang G, Kim Y, Kim J, Ha J. AMPK activators: mechanisms of action and physiological activities. Exp Mol Med. 2016;48:e224.
36. Inoki K, Zhu T, Guan KL. TSC2 mediates cellular energy response to control cell growth and survival. Cell. 2003;115:577–90.
37. Clarke PR, Hardie DG. Regulation of HMG-CoA reductase: identification of the site phosphorylated by the AMP-activated protein kinase in vitro and in intact rat liver. EMBO J. 1990;9:2439–46.
38. Jager S, Handschin C, St-Pierre J, Spiegelman BM. AMP-activated protein kinase (AMPK) action in skeletal muscle via direct phosphorylation of PGC-1alpha. Proc Natl Acad Sci U S A. 2007;104:12017–22.
39. Cao J, Meng S, Chang E, Beckwith-Fickas K, Xiong L, Cole RN, et al. Low concentrations of metformin suppress glucose production in hepatocytes through AMP-activated protein kinase (AMPK). J Biol Chem. 2014; 289:20435–46.
40. Miller RA, Chu Q, Xie J, Foretz M, Viollet B, Birnbaum MJ. Biguanides suppress hepatic glucagon signalling by decreasing production of cyclic AMP. Nature. 2013;494:256–60.
41. Ji L, Faponle AS, Quesne MG, Sainna MA, Zhang J, Franke A, et al. Drug metabolism by cytochrome p450 enzymes: what distinguishes the pathways leading to substrate hydroxylation over desaturation? Chemistry. 2015;21:9083–92.
42. Guengerich FP. Cytochrome p450 and chemical toxicology. Chem Res Toxicol. 2008;21:70–83.
43. Huttunen KM, Mahonen N, Raunio H, Rautio J. Cytochrome P450-activated prodrugs: targeted drug delivery. Curr Med Chem. 2008;15:2346–65.